

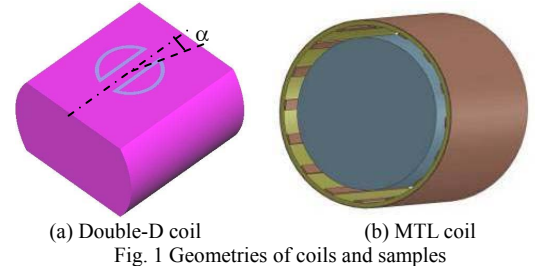
Analysis of equivalent noise resistance of surface and small volume coils by the finite element method

Y. Li¹, Y. Guo¹, and X. Jiang¹

¹Department of Electrical Engineering, Tsinghua University, Beijing, Beijing, China, People's Republic of

Introduction The equivalent noise resistance of RF coils is dominated by the coil self resistance and the sample resistance in the case of surface coils of low field MRI and small size volume coil of extra high field MRI [1], especially animal coils which are integrated with animal holder. In terms of coil self resistance analysis, the accuracy of the current density distribution in the conductor calculated by the finite difference time domain (FDTD) is limited by the Cartesian grid [2] whereas the finite element method (FEM) can achieve accurate results of RF field distribution in both coil conductor and imaging sample. This work proposes an approach to analyze the equivalent noise resistance, including coil self-resistance, of surface coils of low field MRI and small volume coils of extra high field MRI using the FEM. Prototype coils were built to evaluate the simulation results and *in vivo* images were acquired.

Method The simulations of surface coil of low-field MRI and small size volume coil of extra high field MRI were carried out using frequency response analysis of commercial FEM software JMAG 10.0 (JRI Solution, Limited, Japan) since the coil structures were much smaller than the wavelength at resonance frequency. A double-D coil and a microwave transmission line (MTL) coil [3] were taken as examples for surface coil and small size volume coil respectively. The geometries of both coils and samples were shown in Fig. 1. The double-D coil was with a diameter of 165 mm and $\alpha = 16.4^\circ$. The conductors (gray region) were 0.2 mm thickness copper tapes ($\sigma = 5.3 \times 10^7$ S/m, $\mu_r = 1$ and 10 mm in width). The sample (red region, $\sigma = 0.8$ S/m and $\mu_r = 1$) was 400 mm in length with racetrack-shaped cross section. The diameter and height of the racetrack-shaped cross section were 410 mm and 240 mm respectively. A three-dimension FEM simulation was performed at 14.85 MHz which is the proton resonance frequency at 0.35T. Surface impedance boundary condition was set on the surface of conductors in order to reduce meshing scale. The 16 element MTL coil was built on an acrylic tube ($\sigma = 0.001$ S/m and $\mu_r = 1$) of 87 mm inner diameter, 101 mm out diameter and 60 mm length. The conductors (brown region) were 36 μm copper tapes ($\sigma = 5.3 \times 10^7$ S/m, $\mu_r = 1$ and 6.35 mm in width) and the thickness of the substrate was 7 mm. The shield was 36 μm copper film. The sample (blue region, $\sigma = 0.8$ S/m and $\mu_r = 1$) was a cylinder of 50 mm diameter and 60 mm length. A two-dimension FEM simulation was performed at 400.2 MHz which is the proton resonance frequency at 9.4T. Both of the two coils were excited by sinusoidal current with RMS value of 1 A.



(a) Double-D coil (b) MTL coil
Fig. 1 Geometries of coils and samples

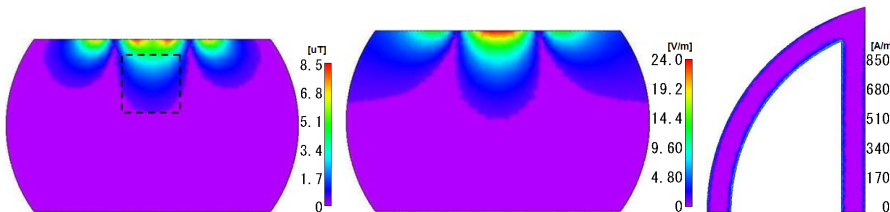


Fig. 2 B1 map, electric field map in the transversal plane of the sample and current density distribution on the surface of conductor of double D coil calculated by JMAG. The dashed box indicated the heart region.

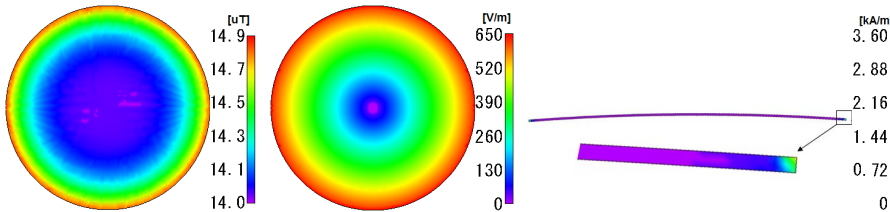


Fig. 3 B1 map, electric field map and current density distribution of MTL coil calculated by JMAG

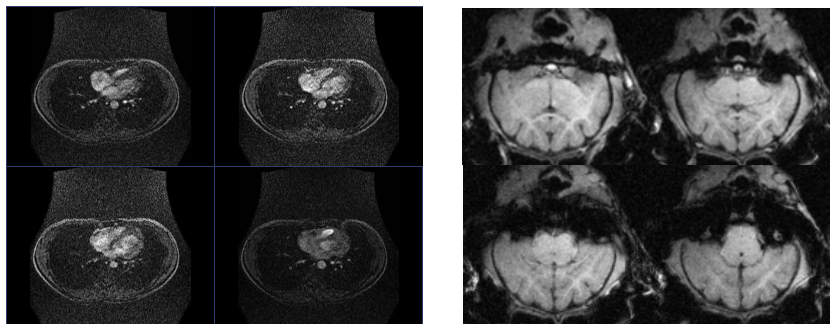


Fig. 4 *In vivo* images of heart acquired with array coil and of cat brain acquired with MTL coil

suggest that the finite element method is feasible to analyze surface coils of low field MRI and small volume coils of extra high field MRI. The coil self-resistance accounts higher percentages of the equivalent noise resistance in these cases.

References 1) T W Redpath. *The British Journal of Radiology*, 1998, 71:704-707; 2) C M Collins. *NMR in Biomedicine*, 2009, 22(9):919-926 3) Y Li, *et al.* 16th annual meeting of ISMRM, 2008, p2984.

Acknowledgments

This work was supported by a grant from the National High Technology Research and Development Program of China (863 Program) (No. 2006AA020802) and the National Natural Science Foundation of China General Program (50777039).

Results The B1, electric field distribution in the transversal planes of sample, and the current density distribution on the conductor were shown in Fig. 2 and Fig. 3. The B1 sensitivity homogeneity of the MTL coil was up to 95%. The coil self-resistance and sample resistance of the double-D surface coil were 81.8 m Ω and 120.6 m Ω respectively, whereas those of the MTL coil were 3.58 Ω and 18.49 Ω respectively. The results indicate the equivalent noise resistance of surface coils of low-field MRI is dominated by both coil self-resistance and sample resistance whereas the coil self-resistance is comparable with the sample resistance in term of small size volume coils in extra high field MRI. A two channel coil array which consisted of a racetrack-shaped Helmholtz coil and the double D surface coil was fabricated. Transversal images of four phases in one cardiac period were acquired *in vivo* on a 0.35T permanent MRI system using spoiled gradient recalled acquisition (SPGR) image sequence with TE = 7.5ms, TR = 13.5ms, flip angle = 30 $^\circ$, FOV = 340 mm \times 340 mm, slice thickness = 5 mm, 256 \times 256 imaging matrix, 0.5 averages, 75% phased encoding. The *in vivo* images in Fig. 4 indicate the sensitivity in the heart region increases by using double-D coil as the simulation results shown in Fig. 2. A prototype MTL volume coil was fabricated and tuned to 400.2 MHz. Four multiple-slice images of cat brain were acquired *in vivo* on a 9.4T/31 cm bore magnet (Magnex Scientific, UK) system interfaced with the Varian INOVA console (Varian Inc., Palo Alto, CA), using GE image sequence with flip angle = 11 $^\circ$, TE = 5 ms, TR = 10 ms, FOV = 8 cm \times 8 cm, 128 \times 128 imaging matrix, 5 averages, slice thickness = 2 mm. The anatomic images shown in Fig. 4 illustrate that the MTL volume coil provides good sensitivity homogeneity in the cat brain, which is coincident with the simulation results shown in Fig. 3.

Conclusion The analysis result and *in vivo* images